Fluorescence Measurements of OH in a Turbulent Flame

M. Azzazy* and John W. Daily†
University of California, Berkeley, California

Laser-induced fluorescence spectroscopy has been used to measure OH concentration probability density functions (PDFs) in a turbulent premixed flame. The methane-air flame is stabilized on a rod flame holder located downstream of a turbulence producing grid. Measurements in both the streamwise and transverse directions have been made for a variety of flow conditions. The PDFs display a single peaked behavior throughout the flame, with the broadest structure in the center of the flame. A simple limit analysis shows that the observed behavior of the PDF is consistent with expected behavior for an intermediate radical specie over the range of flame, optical, and turbulence length scales present in our experiment.

Introduction

THE study of turbulent premixed flames traditionally has been limited by a lack of experimental data that could be of help in closing the governing equations. In recent years, much work has focused on the use of probability density distribution functions (PDFs) of the dependent variables in an attempt to close the turbulent transport equations in a way amenable to experimental verification. It has been shown that a knowledge of PDFs can often greatly simplify the closure problem and lead to practical numerical schemes for predicting flame behavior.

Until now, work has focused on the passive scalars temperature or reaction progress variable. Little has been done to incorporate more realistic chemical kinetics into an experimentally verifiable theory. Since we have the capability of making spatially and temporally resolved OH concentration measurements using laser-induced fluorescence spectroscopy, we felt that measurement of OH PDFs in a turbulent premixed flame would provide both useful data and a feasibility test for the experimental technique.

Concurrently with making the measurements, we have been working on a theoretical model of our flow. To be reported on in detail elsewhere, the model treats reaction kinetics in a two-step mechanism: $R \rightarrow I$ and $I \rightleftarrows P$, where reactants R form intermediates I which react to form products P. The conservation equations are then cast in a form which leads to integrodifferential transport equations for the probability density of each specie. The reactant, intermediate, and product pools are chosen based on the kinetic modeling of Guirgius et al.,[1] who show that OH can be used as a representative specie for the intermediate pool. Thus a measurement of OH PDFs would provide useful data for direct verification of an analytic model.

Laser-induced fluorescence spectroscopy (LIFS) involves the selective excitation of a chemical specie of interest and detection of the resulting fluorescence signal.[2] Under suitable conditions the fluorescence signal resulting from a molecule such as OH can be shown to remain linearly related to concentration over the temperature and mixture variation found in a turbulent flame. Because the focal volume formed at the intersection of the laser beam and collection optics can be quite small, spacial resolution on the order of 0.3 mm is easy to obtain. Furthermore, excitation with a pulsed laser of 1 μs pulse length can provide single-shot data which, when repeated at regular intervals, result in unambiguous PDFs.

In the following, we discuss the experimental aspects of our study. The apparatus is then described. Experimental results are presented and analyzed. The results of our work are then summarized and conclusions stated.

Experimental Considerations

A number of factors involved in the application of LIFS to making measurements in a turbulent flame environment have been discussed in Ref. 3. In this section, we additionally address the effect of appropriate length and time scales on signal interpretation, the relationship between the fluorescence signal and the OH concentration, and the effect of trapping and its correction.

Characteristic Scales

The method of measurement is to focus the laser source into the flame and to collect fluorescence at 90 deg to the laser beam. The focal volume thus formed is approximately 300 μm in its largest dimension. The laser pulses last about 1 μs and are repeatable at a rate of 30/s. A PDF is generated by constructing a signal histogram using some large number of pulses, usually above 1000. If the experimentally obtained PDF is to correspond to the actual OH fine point concentration PDF, then the length and time scales of the turbulent flow and chemical kinetics must be reasonably larger than those mentioned above.

The small-scale structure of the turbulent motion is characterized by the Kolmogorov length and time scales, η and τ_K, respectively

$$\eta = (\nu^3/\epsilon)^{1/4} \tag{1}$$

and

$$\tau_K = (\nu/\epsilon)^{1/2} \tag{2}$$

where ν is the kinematic viscosity and ϵ is the rate of energy dissipation defined as u^3/L. u is the characteristic velocity of the flow and L is the integral length scale[4] characteristic of the large-scale motion.

In general, the integral time scale is of the same order as the time taken to convect a lump of fluid across the largest eddy, that is,

$$\tau_I \sim L/u \tag{3}$$

For grid turbulence, the integral length scale is approximately equal to the grid element spacing δ_g at distances of a few tens of δ_g downstream from the grid. From this and Eq. (3) the other scales can be estimated. The results are given in Table 1.

In premixed hydrocarbon combustion, OH is initially formed in superequilibrium amounts and then decays to the equilibrium value as oxidation of CO occurs (Fig. 1). For

Presented as Paper 82-0239 at the AIAA 20th Aerospace Sciences Meeting, Orlando, Fla., Jan. 11-14, 1982; submitted Jan. 22, 1982; revision received Oct. 7, 1982.

*Research Assistant, Department of Mechanical Engineering. Student Member AIAA.

†Associate Professor, Department of Mechanical Engineering. Member AIAA.

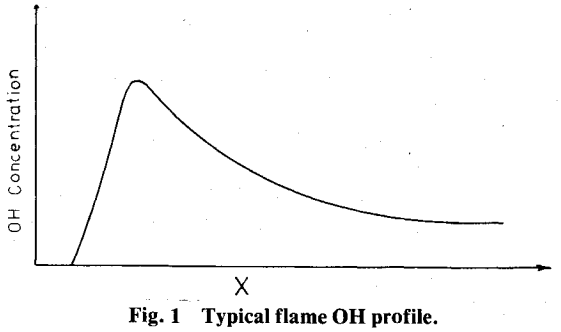

Fig. 1 Typical flame OH profile.

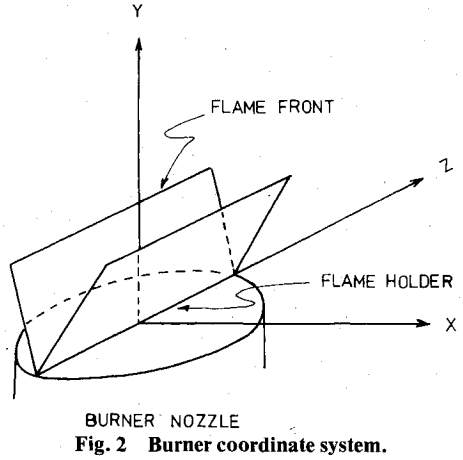

Fig. 2 Burner coordinate system.

homogeneous combustion one can define a characteristic ignition time as τ_{ig}, the time for the OH peak to occur, and a characteristic completion time as τ_c, the time from the peak until equilibrium is reached. For discrete flames there are corresponding length scales. For methane-air the length and time scales are shortest at near stoichiometric equivalence ratios. Approximate values for these scales, presented in Table 1, can be obtained from data on methane-air flames and homogeneous shock tube combustion.[5,6]

One may consider two limits of combustion so as to choose the appropriate scales. In the wrinkled flame limit, the discrete flame will propagate across patches of unburned fluid. Thus the flame thickness and Kolmogorov lengths are the shortest lengths to consider.

For intense turbulence, eddy rollup causes a compression of length scales because of enhanced diffusion. In this case, the shortest length scale is perhaps the Kolmogorov length, which may be interpreted as the shortest distance over which significant gradients are supported.

As can be seen, the laser pulse length is much shorter than any characteristic time, while the focal volume size is of the same order as the Kolmogorov length.

Relationship of the Fluorescence Signal to OH Concentration

The experimentally obtained PDFs are actually those of the fluorescence signal corrected for trapping as outlined below. The signal is related to the total OH number density in a complex fashion which depends on the line pumped, the detection strategy followed, and the rotational, vibrational, and electronic energy transfer rates.

Ideally, one would like to arrange for a linear relationship between the OH number density and the signal. Using the numerical code and energy relaxation rate data of Chan and Daily[7] it was determined that pumping near the peak of the rotational distribution and bandwidth detection would result in a linear relationship within the typical 5-15% precision of our data. These results appear to be valid over the temperature range of our experiment.

Measurements were then made in a flat flame burner for a number of pumps and detected bandwidths. The measurements confirmed the numerical results within the precision of the data. Thus, it is assumed that the fluorescence signal is linearly related to the OH number density.

An absolute calibration was not performed, other than to note that the concentration of OH in the burned gas region of the flame is probably fairly close to the equilibrium value.

Trapping Correction

Both the laser beam and fluorescence experience absorption, or trapping, by the large concentration levels of OH present in our flame. (The flame geometry is illustrated in Fig. 2.) The attenuation of radiation by line absorption is written as

$$I_\nu(s) = I_\nu(0)\,e^{\int_0^s \alpha_\nu(s')\,ds'} \tag{4}$$

where α_ν is the spectral absorption coefficient, I_ν the spectral intensity, and s the distance along the optical path. For a given transition, the spectral absorption coefficient α_ν is

$$\alpha_\nu = h\nu B_{12} n_1 \phi(\nu) \tag{5}$$

where n_1 is the total number density of the ground state, B_{12} the transition probability, ν the transition frequency, h Planck's constant, and $\phi(\nu)$ the normalized line shape function.

In the case of weak absorption, one may expand the exponential term in Eq. (4) and truncate at the second term to yield

$$I_\nu(s) \simeq I_\nu(0)\left[1 - \int_0^s \alpha_\nu(s')\,ds'\right] \tag{6}$$

In our experiment we detect the total intensity I, integrated over a bandwidth $\Delta\nu$. Integrating Eq. (6) yields the total intensity

$$I(s) = \int_{\Delta\nu} I_\nu(0)\left[1 - \int_0^s \alpha_\nu(s')\,ds'\right]d\nu \tag{7}$$

We assume that, for our conditions, the trapping of both the laser and fluorescence can be approximated as

$$I(s) = I(0)\left[1 - C\int_0^s n(s')\,ds'\right] \tag{8}$$

where C is an effective absorption coefficient incorporating all molecular parameters and $n(s)$ is a normalized ground state density profile along the line of sight.

Equation (8) is exact only in the broadband limit. For laser absorption this limit applies because the laser linewidth, ~1.6 Å, is considerably wider than the 0.1 Å linewidth of the pumping transition. For fluorescence, the absorption coefficient in Eq. (5) must incorporate all the lines within the

Table 1 Characteristic scales

Time scales, s				
τ_L	τ_I	τ_K	τ_{ig}	τ_c
10^{-6}	1.4×10^{-2}	5×10^{-3}	1.25×10^{-3}	3.75×10^{-3}
Length scales, m				
δ_L	L	η	δ_{ig}	δ_c
300×10^{-6}	1.4×10^{-3}	260×10^{-6}	0.5×10^{-3}	1.5×10^{-3}

collected fluorescence bandwidth. We merely assume that Eq. (8) holds where $n(s)$ is the normalized total OH ground state population.

To determine C for laser and fluorescence absorption, the following experiment was performed. The burner is first positioned so that the laser beam is parallel to the flame holder and stationed vertically above it. The laser attenuation is measured as a function of distance y above the flame holder. Also, at each vertical position the fluorescence is measured as a function of distance along the flame holder or laser beam.

From the laser attenuation measurements one obtains an overall absorption coefficient defined as

$$I_L(D)/I_L(0) = 1 - C_0 D$$

where I_L is the laser intensity and D the burner diameter. If one assumes that the number density of OH is constant along the laser beam, then $C_0 = C_L n(y)$ where $n(y)$ is the centerline normalized number density above the flame holder and C_L is the effective trapping coefficient for the laser. That n does not vary with distance along the flame holder is born out by an observed linear variation of the fluorescence along the laser beam.

From the slope of fluorescence vs distance along the laser beam one obtains the effective trapping coefficients, C_F, for fluorescence.

The burner is then rotated 90 deg and fluorescence data taken at various horizontal and vertical locations. The data result in uncorrected PDFs and mean profiles. To perform the trapping correction we start with an uncorrected mean profile, assuming it to be proportional to $n(x,y)$. This is used to correct for laser absorption. The same profile is then used to correct for fluorescence absorption. In this way, a new profile is constructed point by point in the x,y plane. The process is then repeated until the iteration converges.

The major assumption of the correction is that both laser beam and fluorescence are absorbed by the mean OH number density profile. Because of the burner configuration there would have to be a very large correlation length scale for this assumption to break down. The integral scale is, in fact, only 1.4 mm.

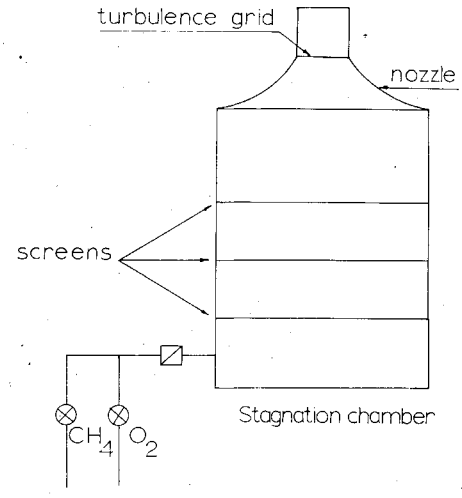

Fig. 3 Burner assembly.

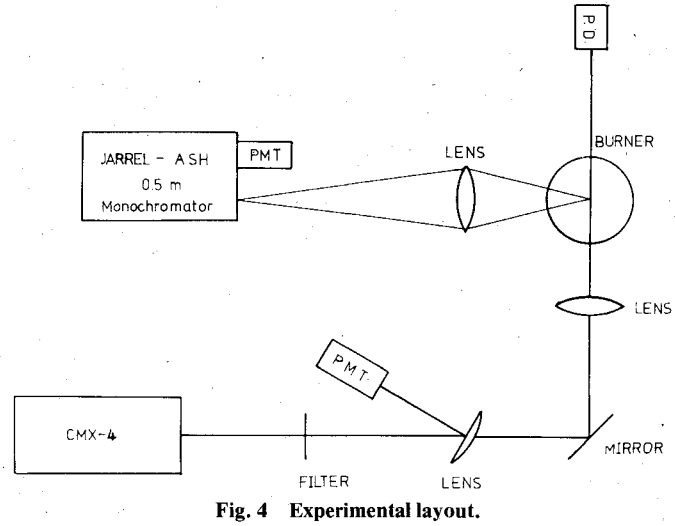

Fig. 4 Experimental layout.

Experimental Apparatus

Burner

The burner is illustrated in Fig. 3. The assembly consists of double stagnation chambers feeding coaxial nozzles. The inner chamber and nozzle carry premixed methane-air reactants, while the outer nozzle is supplied with air.

The inner stagnation chamber is divided into sections by 200-500 mesh screening for turbulence damping. The reactant mixture is then accelerated through a 16:1 contraction. Air flowing in the outside nozzle acts as a shield to minimize outside entrainment and jet mixing effects on the flame. The mass flow rates are monitored by three sets of four sonic nozzles with different diameters to allow for a wide dynamic range.

Turbulence is generated by a square grid placed on top of the coaxial nozzles. The grid has a mesh spacing of 2.8 mm and wire diameter of 0.5 mm. The methane-air flame is stabilized on a 0.132 cm rod located 5 cm downstream of the grid forming in a "V" shape.

Two computer controlled stepping motors were used for the horizontal and vertical displacement of the burner. The burner displacement was measured using a Sony Magnescale linear displacement transducer which has a resolution of 1 μm.

Optical Arrangement

Figure 4 illustrates the experimental layout. A frequency doubled Chromatix CMX-4 flash lamp pumped dye laser is tuned to the appropriate absorption line of OH. We pump the $Q_1(4)$ line of the $A^2\pi \rightarrow X^2\Sigma^+$ electronic transition at 3083 Å. The laser line width was 1.6 Å. The pulse, of about 1 μs duration, is focused to a waist diameter of 0.3 mm in the flame with a two-lens system. Light reflected from the back of the first lens is directed to a photomultiplier tube to monitor the laser power while a PIN diode placed on the far side of the flame is used to measure laser beam attenuation.

The fluorescence signal is collected at 90 deg to the laser beam and imaged onto the entrance slit of a 0.5-m Jarrel-Ash monochromator with F/3.5 optics. The monochromator entrance and exit slits are set at 1 and 3 mm, respectively, resulting in a 48-Å bandpass. The monochromator is centered at 3083 Å, which mainly admits the Q_1 band. A photomultiplier placed at the exit slit is used to monitor the fluorescence signal.

The collection optics image the entrance slit of the monochromator to 0.33 mm at the laser focal volume. Thus, the spatial resolution is defined by a disk about 0.3 mm in diameter and 0.33 mm thick.

Signal Processing

The signals from the two photomultipliers or the power monitoring PMT and the PIN diode are input into a two-channel gated integrator which is interfaced to a DEC LSI-11 microprocessor. The signal of interest is normalized by the laser power and stored until enough points have been collected to form a PDF.

The PDF is constructed by counting the number of times the signal falls within a given interval, the entire signal range being divided into equal intervals or bins. The ratio between the number of entries in each bin to the total number of observations yields a discretized probability density function.

Uncertainty

The final product of our measurements are the PDFs themselves and various moments calculated from the PDFs. Uncertainty exists in these quantities because of uncertainty in the single-shot values of the signal and because of resolution limitations and the resulting statistical uncertainty in constructing the PDFs.

Uncertainty in the single-shot measurements arises from photon counting laser power fluctuations, beam wander, noise in the detection and processing electronics, radiative trapping, and lack of linearity.

The uncertainty attributed to laser power fluctuations, beam wander, and electronic noise was experimentally determined to be 1.6% of the full-scale signal level. Full scale corresponds to about 5×10^4 photoelectron/pulse or a statistical uncertainty of 0.4%, at 10 and 1% full scale, the uncertainty becomes 1.3 and 4.5%, respectively. The major source of uncertainty lies in lack of linearity and uncertainty regarding the trapping corrections. We estimate these to be about 10% of each single-shot value.

Regardless of uncertainty in single-shot measurements, the statistical precision of the discrete PDF is limited by the bin size and the number of points in each bin. The statistical precision is inversely proportional to the square root of the number of entries for each bin. Therefore, for a specific total number of data points, the bin size must be chosen in a way to minimize the statistical uncertainty while maintaining satisfactory resolution. Thus the average number of entries in

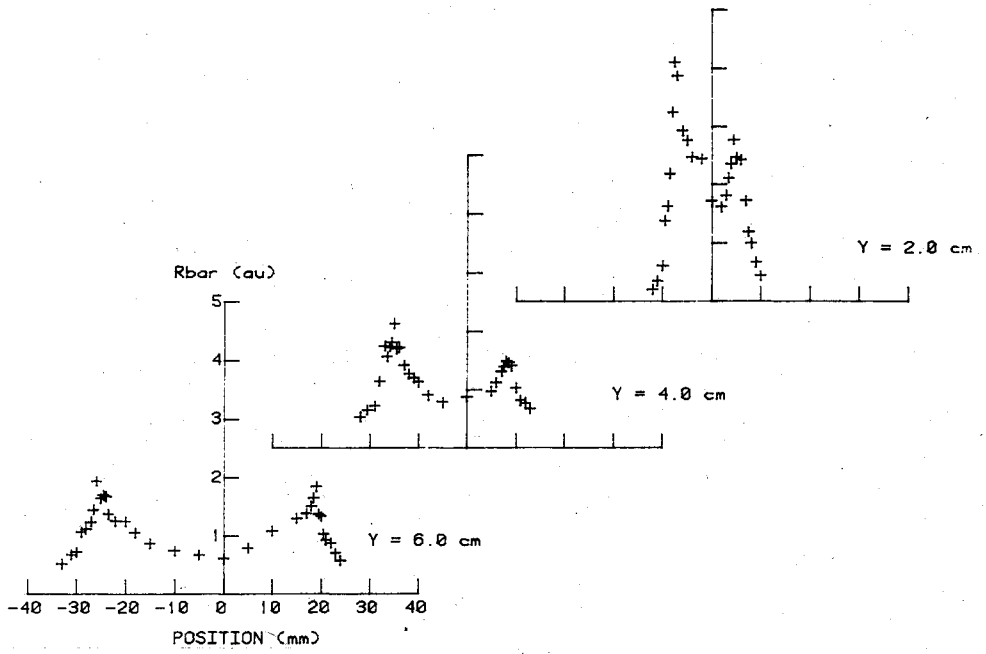

Fig. 5 Mean concentration profiles ($U=2$ m/s, $\phi=0.6$).

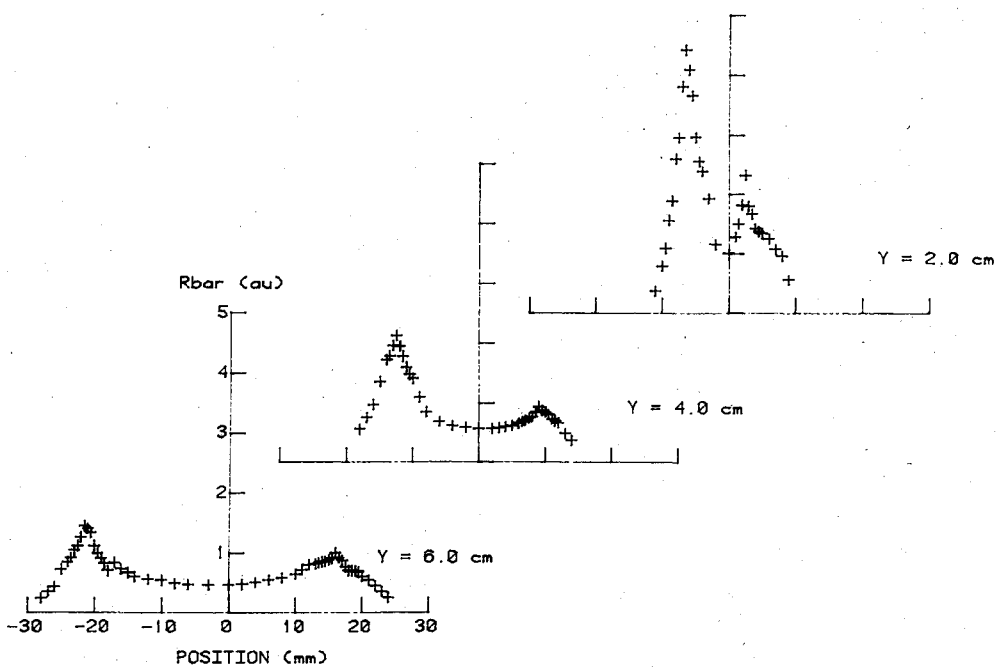

Fig. 6 Mean concentration profiles ($U=4$ m/s, $\phi=0.75$).

each bin is about 12, leading to an average bin uncertainty of 3%, which is less than our estimate of about 10% for single-point statistical uncertainty.

Experimental Results

Results are reported here for two upstream velocities, $U=200$ and 400 cm/s. The equivalence ratio ϕ was varied in such a way to be the minimum for flame stabilization. The equivalence ratios reported are 0.6 and 0.75 corresponding to flame half cone angles of 20.5 and 18 deg, respectively. Data records were taken at 2, 4, and 7 cm above the flame holder and every 0.5 mm apart across the flame fronts. Each data record was used to construct a PDF and calculate the mean and standard deviation of the signal. The data for all conditions was normalized to the centerline mean value at $y=2$ cm and $U=400$ cm/s.

Mean concentration profiles for the two flames are presented in Figs. 5 and 6. The concentration is zero at distances far from the flame, peaks in the middle of each flame front, and drops to a low, perhaps equilibrium value on the hot side. The data show that the flame was not symmetric; that is, the two sides of the V were dissimilar and that the centerline OH concentration dropped with distance above the flame holder. The asymmetry is consistent with density measurements in the same burner and is not an artifact of the fluorescence trapping.

Profiles of rms concentration fluctuations normalized on the centerline mean value are shown in Figs. 7 and 8. The fluctuations can also be normalized on the local mean value

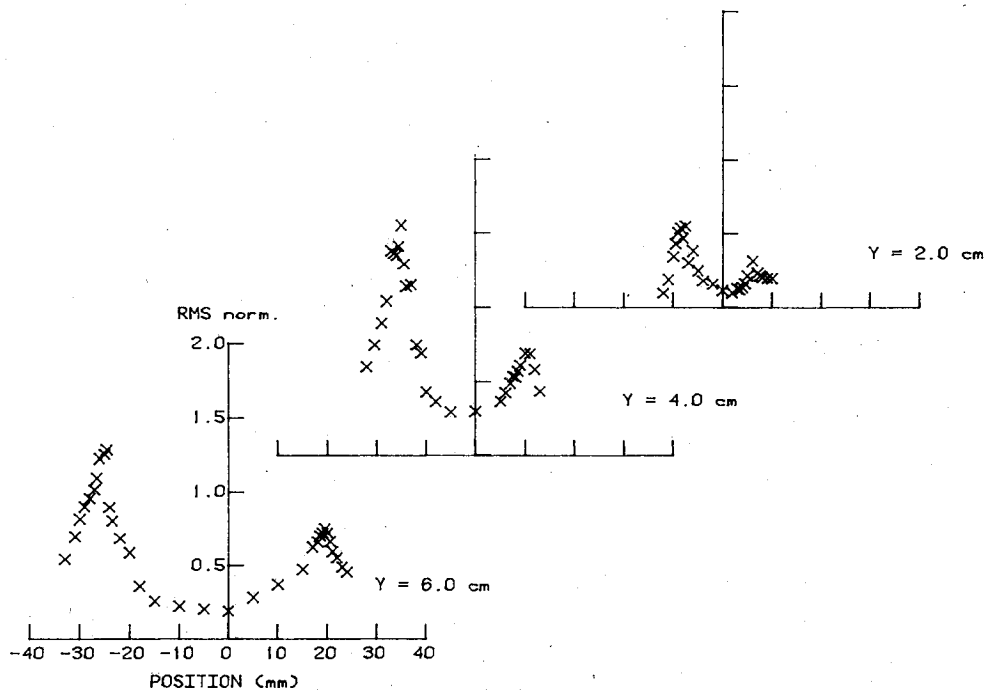

Fig. 7 rms concentration profiles normalized on the mean centerline value ($U=2$ m/s, $\phi=0.6$).

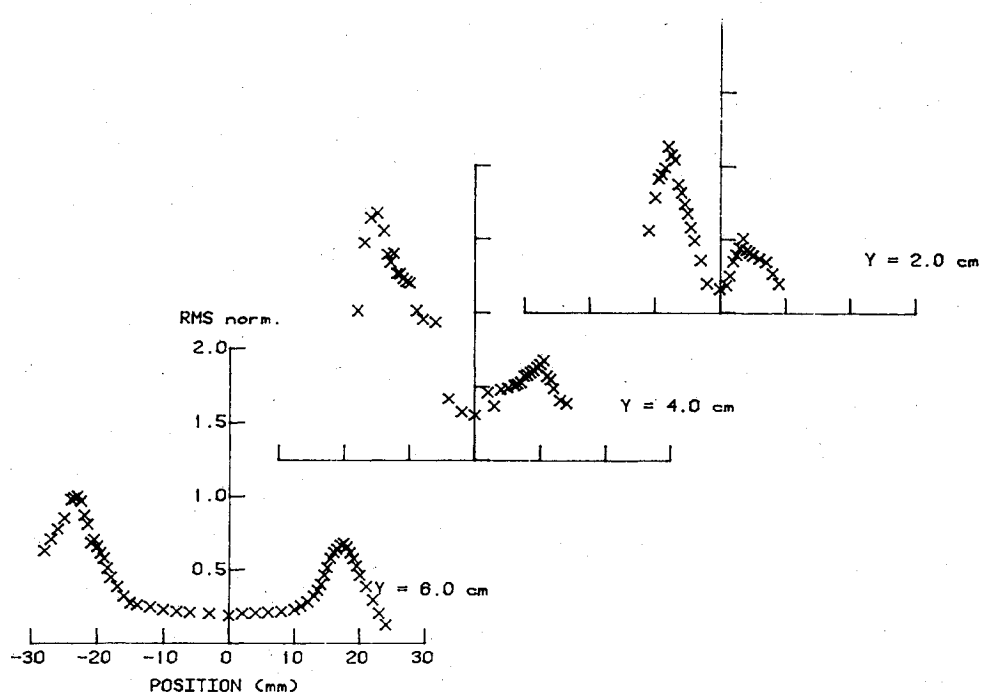

Fig. 8 rms concentration profiles normalized on the mean centerline value ($U=4$ m/s, $\phi=0.75$).

and plotted as shown in Figs. 9 and 10. Interestingly, the percent fluctuation curves peak close to the cold side of the flame. They are also very sensitive to any glitches in the mean profile. Since the mean OH concentration is rapidly falling on the cold side, using the local mean to normalize the rms may not be an appropriate way to present the data. Not surprisingly, the fluctuations peak in the flame zone where there is vigorous reaction and mixing.

Figure 11 shows the PDFs at various flame locations. On the cold side of the flame, the PDF appears as a delta function with a relatively broad tail. The delta function appears because of the large amount of unburnt reactants which are present, while the tail reflects the occasional excursion of hot gases past the focal volume. Deeper into the flame the average OH concentration increases and the PDF becomes more Gaussian centered around the mean and changes a relatively large standard deviation. Turbulence fluctuations are responsible for broadening the Gaussian-like distribution of the PDF as turbulent motion feeds the focal volume with gases having different OH concentrations. At the hot side of the flame the PDF is again a Gaussian-like shape with a smaller standard deviation and peaking at what appears to be the equilibrium OH concentration. As the measuring station moves away from the flame front the OH concentration drops and only hot gases are mixed, which decreases the standard deviation.

The observed PDFs are consistent with what we expected the actual fine point PDFs to look like. Under circumstances

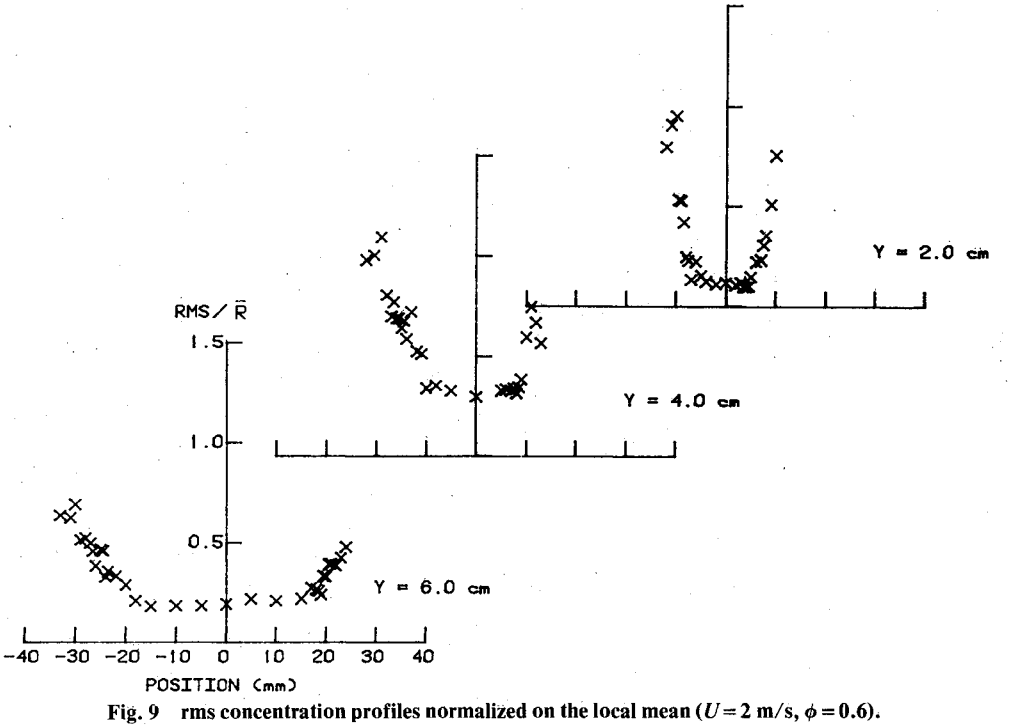

Fig. 9 rms concentration profiles normalized on the local mean ($U = 2$ m/s, $\phi = 0.6$).

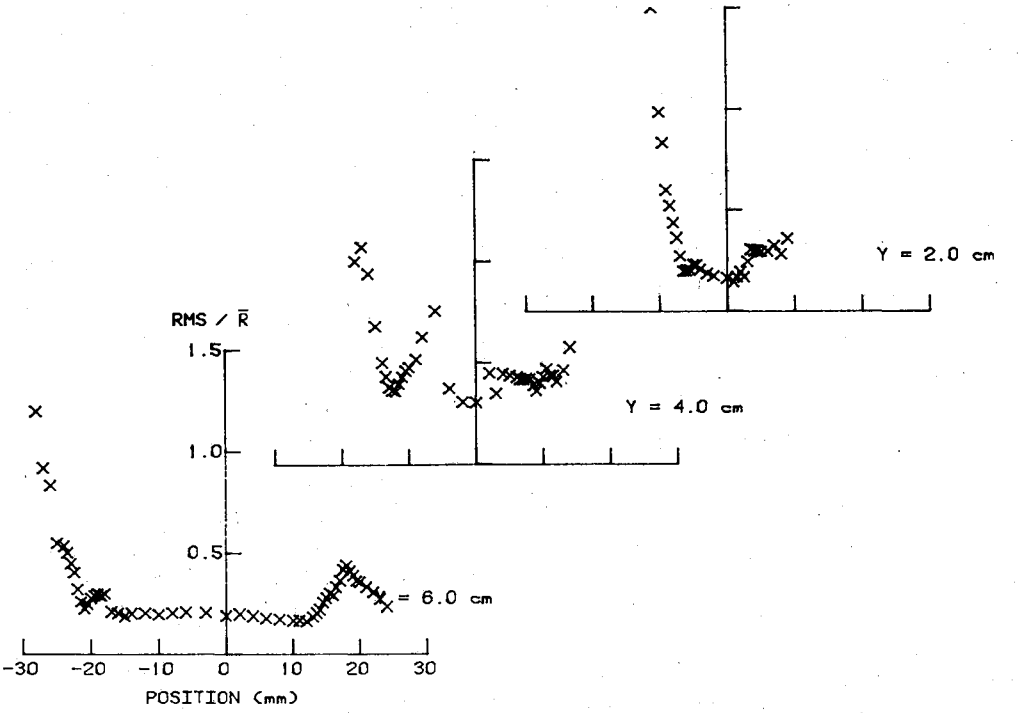

Fig. 10 rms concentration profiles normalized on the local mean ($U = 4$ m/s, $\phi = 0.75$).

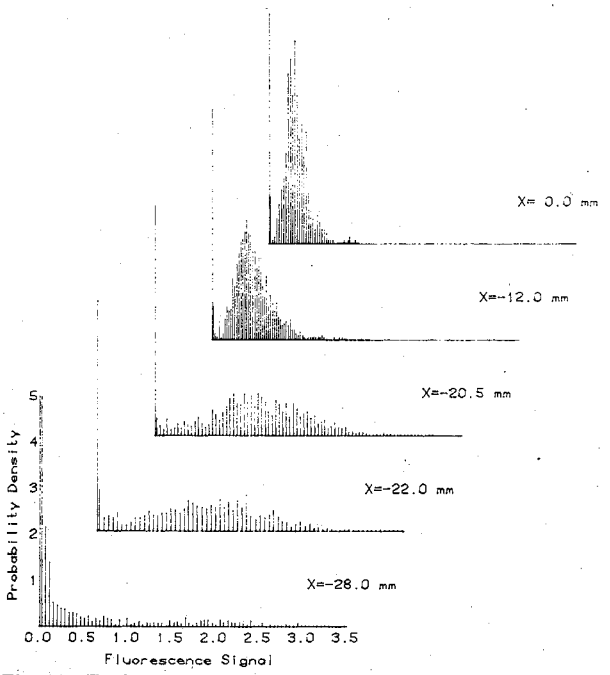

Fig. 11 Typical PDFs of OH concentration ($U = 4$ m/s, $\phi = 0.75$).

which would produce a bimodal distribution of a scalar-like density or reaction progress variable, the OH PDF will have the distribution weighted significantly because of convolution with a function such as shown in Fig. 1. Thus, even though one expects bimodal density PDFs, as shown by Bill et al.[8] in a similar flame, OH will not display such behavior.

Summary and Conclusions

Laser-induced fluorescence spectroscopy has been used to measure OH PDFs in a plane flame propagating into grid turbulence. The results show single-peaked PDFs throughout the flame, with the broadest structure in the center of the flame zone. The measurement method is shown to be a practical and effective way of obtaining radical species measurements in real flame environments.

Acknowledgments

This work was supported by Air Force Office of Scientific Research Grants 77-3357 and 81-022. Dr. Robert Bill provided drawings for the burner and participated in many useful discussions.

References

[1] Guirguis, R. H., Oppenheim, A. K., Karasola, I., and Creighton, J. R., "Thermochemistry of Methane Ignition," Presented at the 7th ICOGER, Gottingen, Federal Republic of Germany, 1979, p. 134.

[2] Daily, J. W., "Laser Induced Fluorescence Spectroscopy in Flames," ACS Symposium Series 134, *Laser Probes for Combustion Chemistry*, 1980, p. 61.

[3] Daily, J. W., "Detectability Limit and Uncertainty Considerations for Laser Induced Fluorescence Spectroscopy in Flames," *Applied Optics*, Vol. 17, 1978, p. 1610.

[4] Tennekes, H. and Lumley, J. L., *A First Course in Turbulence*, MIT Press, Cambridge, Mass., 1977.

[5] Tsatsaronis, G., "Prediction of Propagating Laminar Flames in Methane, Oxygen, Nitrogen Mixtures," *Combustion and Flame*, Vol. 33, 1978, p. 217.

[6] Cooke, D. F. and Williams, A., "Shock Tube Studies of the Ignition of Ethane and Slightly Rich Methane Mixtures with Oxygen," *Thirteenth Symposium (International) on Combustion*, The Combustion Institute, Pittsburgh, Pa., 1977, p. 757.

[7] Chan, C. and Daily, J. W., "Laser Excitation Dynamics of OH in Flames," *Applied Optics*, Vol. 19, 1980, p. 1357.

[8] Bill, R. G., Namer, I., Talbot, L., and Robben, F., "Density Fluctuations of Flames in Grid-Induced Turbulence," *Combustion and Flame*, Vol. 44, 1982, p. 277.